Hydrogenation of *p*-Chloronitrobenzene on Ni-P-B Nanoalloy Catalysts

Wei-Jye Wang,[†] Jia-Huei Shen,[‡] and Yu-Wen Chen*[,‡]

Department of Chemical Engineering, Far-East College, Tainan 605 Taiwan, and Department of Chemical Engineering, Nanocatalysis Research Center, National Central University, Chung-Li 320 Taiwan

A series of nanosized NiPB amorphous alloy catalysts with various concentrations was prepared by chemical reduction of nickel acetate with sodium hypophosphite and sodium borohydride in aqueous solution at 298 K under N_2 curtain gas with vigorous stirring. The catalysts were characterized with inductively coupled plasma-atomic emission spectroscopy, nitrogen sorption, X-ray diffraction, transmission electron microscopy, and X-ray photoelectron spectroscopy. The catalysts were tested for liquid-phase hydrogenation of *p*-chloronitrobenzene at 1.2 MPa hydrogen pressure, 353 and 393 K reaction temperature, absolute ethanol as a reaction medium, 500 rpm stirring speed, 0.2 M *p*-CNB, and 2 mmol of Ni catalyst. The initial Ni/P/B molar ratio of starting materials affected the concentration of boron and phosphorus bound to the nickel metal, resulting in a change of surface area, amorphous structure, and hydrogenation activity of the catalyst. The XPS results revealed that boron combined with nickel metal in the NiPB powder donates electrons to nickel metal and that phosphorus withdraws electrons from nickel metal. The sample NiPB(1:3:3) (the values in parentheses are Ni/P/B ratios in the starting materials) prepared at 298 K under N_2 flow with vigorous stirring had the highest surface area of 28.2 m^2/g. The BET surface area increased with an increase of phosphorus content in the sample. The XPS results revealed that boron could donate electrons to the nickel metal and that phosphorus could accept electrons from the nickel metal in the NiPB catalysts. By regulating the concentrations of boron and phosphorus, one could regulate the electron denisity of nickel, which in turn could influence the activity of the catalyst. The order of activity per weight of the catalyst was NiPB(1:0.3:3) > NiPB(1:1:3) > NiB(1:3) > NiPB (1:3:3). The activities per surface area and turnover frequencies of the catalysts also decreased in the same order. NiPB catalysts prepared with suitable Ni/P/B ratios in the starting materials had higher activities than the NiB catalyst. Small amounts of phosphorus in the NiB catalyst can increase the surface area and turnover frequency. Both are beneficial for promoting the reaction. However, an overdose of phosphorus became a poison for the Ni catalyst.

1. Introduction

Ultrafine materials have attracted extensive interest in recent years,[1−12] owing to their unique isotropic structural and chemical properties. Previous investigators reported that the ultrafine materials can create novel physical, mechanical, and chemical properties, particularly for catalytic and magnetic recording applications.[1,13,14] Okamoto et al.[14−16] characterized the surface of NiB and NiP ultrafine catalysts prepared by a chemical reduction method with X-ray photoelectron spectroscopy (XPS), indicating that a variation in 3d electron density on the nickel metal induced by boron or phosphorus would modify the activity and selectivity of the nickel catalyst for hydrogenation. The nanocatalysts have more surface atoms and a higher concentration of highly coordinated unsaturated sites. A nanosized Ni catalyst modified with boron has been reported to be a good catalyst for hydrogenation of nitrobenzene and furfural.[17−21] The catalytic properties are highly dependent upon the preparation method.[22,23] Many systematic studies have been made on catalytic properties for Ni−B catalysts.[24−31]

In contrast, very few studies have been devoted to Ni−P−B catalysts. Shen et al.[12] successfully prepared NiPB ultrafine amorphous particles by chemical reduction methods. As generally known, boron or phosphorus will affect the surface properties of these catalysts and their catalytic properties. The NiPB ultrafine amorphous alloy powders, which consist of two metalloid elements (B, P) and the feature of ultrafine amorphous structure, have seldom been studied in their surface state and for application in catalytic reactions. Our previous investigations[23,32] indicated that the Ni/P/B molar ratios in the starting material significantly affected the concentrations of boron and phosphorus bonded to the nickel metal, subsequently affecting the hydrogenation activity and selectivity of the catalyst. The electron transference between nickel and metalloid in the NiPB powder is complex. The different electron transferences between nickel and metalloid elements (boron donates electrons and phosphorus draws electrons) exist at the same time.

Aromatic haloamines are important materials in the chemistry of dyes, pharmaceuticals, pesticides, and herbicides. Because of environmental pollution caused by traditional production methods, many researchers try to make haloamines with selective hydrogenation. However, the hydrogenation of halonitrobenzene is very complicated. Taking *p*-chloronitrobenzene as an example, its N═O group may be hydrogenated or it may be dehalogenated (Scheme 1). Yu et al.[33] have reported the selective hydrogenation of *o*-chloronitrobenzene to *o*-chloroaniline on Pt catalysts. Besides the desired product *o*-chloroaniline, many byproducts such as aniline, nitrobenzene, *o*-chlorophenylhydroxylamine, *o*-chloronitrosobenzene, azo- and azoxydichlorobenzenes, chlorobenzene, and so on were formed at the same time.

Hydrogenation of *p*-chloronitrobenzene (*p*-CNB) has been known to be an important industrial process. It is usually catalyzed by two classes of solids: noble metals, such as platinum, palladium, ruthenium, and rhodium, and Raney

* To whom all correspondence should be addressed. Tel: 886-3-4227151, ext. 34203. Fax: 886-3-4252296. E-mail: ywchen@cc.ncu.edu.tw.

[†] Far-East College.

[‡] National Central University.

10.1021/ie0605736 CCC: $33.50
Published on Web 11/23/2006

Scheme 1

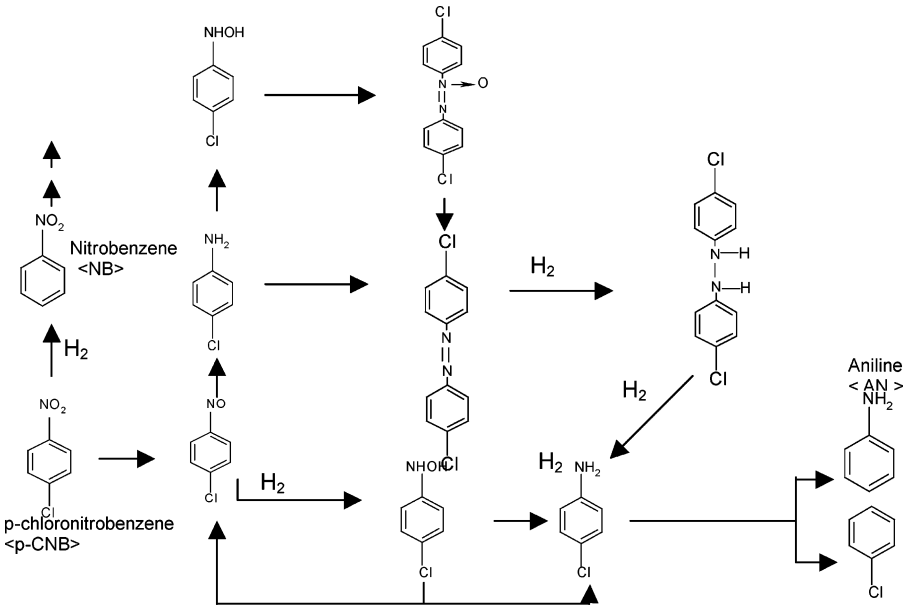

nickel.[34−36] In a previous paper,[23,32,37,38] one of the authors reported that the NiB catalyst is active for the hydrogenation of nitrobenzene and *p*-chloronitrobenzene. It is expected that NiPB would be active for the hydrogenation of *p*-CNB. It is interesting to investigate the effect of compositions of starting materials on the catalytic properties of NiPB.

In this study, a series of nanosized NiPB amorphous alloy catalysts was prepared with various compositions of starting materials by the chemical reduction method. The NiB catalyst was included for comparison. The catalysts were characterized by inductively coupled plasma-atomic emission spectroscopy (ICP-AES), nitrogen sorption, X-ray diffraction (XRD) transmission electron microscopy (TEM), and X-ray photoelectron spectroscopy (XPS). The catalysts were tested for liquid-phase hydrogenation of *p*-CNB.

2. Experimental Procedures

2.1. Materials. *p*-CNB, with a purity of >99%, was obtained from Acros (Belgium). High purity hydrogen gas (>99.99% from Air Product) was used without further purification. Nickel acetate tetrahydrate (>98%) was supplied by Showa Chemicals (Tokyo, Japan). Sodium hypophosphite (>99%) was obtained from Fisher (Pittsburgh, PA). Sodium borohydride (>99%) was purchased from Lancaster (Morecambe, UK). Methanol (>99.9%) was purchased from Tedia Co. (Fairfield, OH). Water was double-distilled.

2.2. Catalyst Preparation. The nanosized NiPB amorphous alloy catalysts were prepared by chemical reduction of nickel salt by hypophosphite and borohydride in the solution at room temperature. A series of NiPB catalysts with various compositions was prepared by mixing 50 vol % methanol in a deionized water solution of nickel acetate (20 mL, 0.1 M) and sodium hypophosphite (1 M) at 298 K under vigorous magnetic stirring. The solution of sodium borohydride (6 mL, 1 M) was then added dropwise with a microtubing pump into the mixture under a nitrogen stream. The atomic ratio of Ni/B in the starting materials was kept at 1:3 in this study to fully reduce the nickel cation to nickel metal. Various Ni/P ratios in the starting materials were used in this study. The black precipitates that subsequently formed were washed thoroughly with deionized water 3 times and with absolute ethanol twice. The samples were blow-dried at room temperature before proceeding with characterization. The catalyst was denoted as NiPB(*x*:*y*:*z*), where *x*:*y*:*z* is the atomic ratio of Ni/P/B in the starting materials.

2.3. Catalyst Characterization. Elemental analysis with inductively coupled plasma-atomic emission spectroscopy (ICP-AES, Jobin-Yvon, France, JY-24) was performed for the catalysts. In general, the weighted samples were dissolved in nitric acid and diluted with distilled water to the concentrated ion within the calibration range of each element. The standard solutions purchased from Merck were diluted and used to establish the calibration curves. Wavelengths in nanometers used for elemental analysis were 231.604, 214.914, and 249.773 for Ni, P, and B, respectively.

The BET surface area was measured by nitrogen volumetric adsorption (Micromeritics ASAP 2010) at −196 °C. The temperature of the liquid nitrogen bath was checked by a thermistor probe. XRD measurements were taken using a Siemens D500 powder diffractometer with Cu− Kα radiation (40 kV, 30 mA). The sample was scanned over the range $2\theta = 5-60^\circ$ to identify the amorphous structure. The morphologies and particle sizes of the samples were determined by TEM performed on a Jeol JEM-1200 EX II electron microscope operating at 160 kV. After an etching of the surface by Ar^+ ions for 15 min, the XPS spectra were recorded with a Thermo VG Scientific Sigma Probe spectrometer using Al Kα radiation (20 kV and 30 mA). The base pressure in the analyzing chamber was maintained on the order of 10^{-9} Torr. The spectrometer was operated at 23.5 eV pass energy. The catalyst sample was mounted quickly onto a grid attached to a sample holder, keeping the powder soaked in 99% ethanol to minimize the oxidation of the powder by air. After evacuating the ethanol, the sample was transferred to the analyzing chamber.

2.4. Catalytic Activity Measurement. All the experiments were carried out in a cylindrical stirred-tank reactor (Parr Instrument Model 4842) with 160 mL capacity. A four-bladed pitched impeller was placed for effective agitation, and the agitator was connected to an electric motor with a variable speed up to 1700 rpm. A pressure transmitter and an automatic temperature controller were also provided. The gases were supplied from cylinders and introduced to the base of the reactor; another tube served as a sampling tube for the liquid phase.

Table 1. Characteristics of the Ni−P−B Catalysts

catalyst	bulk composition (atomic ratio)	surface composition (atomic ratio)	atomic ratio (bulk)	atomic ratio (surface)	Ni/B (atomic ratio)	Ni/(P + B) (atomic ratio)	surface area (m^2/g)	particle size (nm) TEM	particle size (nm) estimated from surface area[a]
(A) NiB(1:3)	$Ni_{83.1}P_0B_{16.9}$	$Ni_{90.5}P_0B_{9.5}$	$NiB_{0.2}$	$NiB_{0.1}$	4.9	4.917	20.3	6.5	33.2
(B) NiPB(1:0.3:3)	$Ni_{69.4}P_{1.0}B_{29.6}$	$Ni_{79.8}P_{0.9}B_{19.3}$	$NiP_{0.014}B_{0.426}$	$NiP_{0.011}B_{0.242}$	2.3	2.268	22.7		29.7
(C) NiPB(1:1:3)	$Ni_{71.2}P_{11.3}B_{17.5}$	$Ni_{73.7}P_{8.0}B_{18.3}$	$NiP_{0.16}B_{0.246}$	$NiP_{0.11}B_{0.248}$	4.1	2.472	23.4	5.7	28.8
(D) NiPB(1:3:3)	$Ni_{60.8}P_{17.3}B_{21.9}$	$Ni_{52.7}P_{34.3}B_{12.3}$	$NiP_{0.284}B_{0.36}$	$NiP_{0.65}B_{0.233}$	2.8	1.55	29.5	26.2	22.9

[a] Estimated by surface area using equation $d(\text{nm}) = (6/S_{BET}\rho) \times 10^3$.

The catalytic activities of the samples were tested by the *p*-chloronitrobenzene (*p*-CNB) liquid selective hydrogenation reaction. The reactor was charged with 2 mmol of Ni catalyst and 2.52 g of *p*-CNB in 80 mL of absolute ethanol solution. Air was flushed out of the reactor with hydrogen at room temperature, and hydrogen was then fed into the reactor. The inlet valve was closed, and heating commenced with stirring (100 rpm) to avoid settling of the catalyst. When the designated temperature was reached, hydrogen was fed to the predetermined pressure (1.2 MPa) (time zero) that was maintained throughout the reaction, and the stirring speed was 500 rpm. During the run, samples were withdrawn periodically (10 min) and analyzed by a gas chromatograph. A gas chromatograph equipped with a flame ionization detector and a 3 m × 1/8 in. (1 in. = 2.54 cm) stainless steel column packed with 5% OV-101 on Chromsorb WAW-DMSC (80−100 mesh) were used for sample analysis in the hydrogenation of *p*-CNB.

3. Results and Discussion

3.1. Catalyst Characterization. Table 1 lists the compositions, surface areas, and particle sizes of the catalyst samples. The compositions on the surface of the samples were determined by XPS, and those of the bulk were determined by ICP-AES. The composition of the starting materials significantly influenced the morphology and particle size of the NiPB amorphous catalysts, subsequently affecting the surface areas of the catalysts. The sample D NiPB (1:3:3) had the largest surface area (29.5 m^2/g). The surface area decreased in the order (D) NiPB (1:3:3) (29.5 m^2/g) > (C) NiPB (1:1:3) (23.4 m^2/g) > (B) NiPB (1:0.5:3) (22.7 m^2/g) > (A)$NiB_{(1:3)}$ (20.3 m^2/g). The experimental results revealed that the BET surface areas increased with an increase of phosphorus content in the sample. All the catalysts were easily degraded by gaseous oxygen; therefore, catalysts should be prepared under nitrogen flow. However, the presence of P and B passivated the surface, and therefore, the catalysts could not ignite in the air.

Since the particles of the catalysts are spherical and nonporous, the average particle size can be estimated by $d(\text{nm}) = (6/S_{BET}\rho) \times 10^3$, where S_{BET} is the surface area and ρ is the density of the particle using the value of 8.9 g/cm^3 (the density of nickel). Since the surface contained boron and phosphorus, one could obtain the surface area of nickel simply by the extraction of the surface areas of boron and phosphorus. The average particle sizes calculated from surface areas were in the range of 22.9−33.2 nm, all in a nanosize range. It should be noted that these average particle sizes were over-estimated for the uncalcined samples because the catalysts were pretreated at 120 °C for 24 h before nitrogen sorption measurements, which would cause metal aggregation and/or sintering to some extent. This is also part of the reason why nitrogen sorption measurements gave different particle sizes from TEM observations.

The stoichiometry for NiPB powders has been attributed to the mechanism of the two competing reactions between metalloids ($H_2PO^-_2$, BH^-_4) and nickel ion (Ni^+)[12]

$$2H_2PO_2^- + 2H_2O + Ni^{2+} \rightarrow Ni\downarrow + H_2\uparrow + 4H^+ + 2HPO_3^{2-} \quad (1)$$

$$4BH_4^- + 2Ni^{2+} + 9H_2O \rightarrow Ni_xB\downarrow + 3H_3BO_3 + 12.5H_2\uparrow \quad (2)$$

In synthesis, the composition was determined by the relative rates of reactions 1 and 2. Therefore, it is possible that the rate of the two reactions did not remain constant throughout the reaction process. However, the difference was not great. It should be noted that all of the nickel was precipitated and that only very small amounts of boron and phosphorus were in the catalyst. Excess amounts of boron were used in this study to obtain the full reduction of nickel.

The Ni/P/B atomic ratios in the bulk of these samples are listed in Table 1. In the sample NiB(1:3), 6.67% of boron has precipitated, and 93.33% of boron has run off. In the sample NiPB(1:0.3:3), 14.2% of boron has precipitated, and 85.8% has ruoff. In the sample NiPB(1:1:3), 8.2% of boron has precipitated, and 91.8% has run off. In the sample NiPB(1:3:3), 4.2% of boron has precipitated, and 95.8% has run off. There is an increase in the precipitating capacity of boron in the sample NiPB(1:0.3:3) and NiPB(1:1:3), although some phosphorus was added in the samples. In other words, adding the proper amount of phosphorus can help the boron to precipitate. The precipitation of boron in the sample NiPB(1:3:3) (4.2%) was less than that in the sample NiB(1:3) (6.67%), inferring that it maybe due to excessive phosphorus.

The typical XRD patterns of the prepared samples as shown in Figure 1 gave only a broad peak around 45° 2θ. This was assigned to the amorphous state of the nickel−metalloid alloy.[13,39] Notably, the patterns contained no distinct peak corresponding to a crystalline phase of nickel, boron, and phosphorus.

The XPS spectra of NiPB samples are shown in Figure 2. The surface compositions of samples determined by XPS are listed in Table 1. In general, nickel is enriched on the surface, although the difference is very small.

The binding energy of the $Ni_{2p3/2}$ level for sample NiB(1:3) (853.6 eV), sample NiPB(1:0.3:3) (853.3 eV), and sample NiPB-(1:1:3) (853.3 eV), as compared with the binding energy of pure nickel metal 852.2 eV, is ascribed to metallic Ni.[15,16,22]

In the B_{1s} level, there are two kinds of boron species on the surface of all the NiPB samples. The peaks around 188.4−188.7 and 192.6−192.7 eV are assigned to the elemental boron and oxidized boron, respectively.

In comparison with the binding energy of pure boron (187.1 eV), the binding energy of all the NiPB samples (188.4−188.7 eV) shifted positively by 1.3−1.6 eV, indicating that boron donates part of its electrons to nickel.

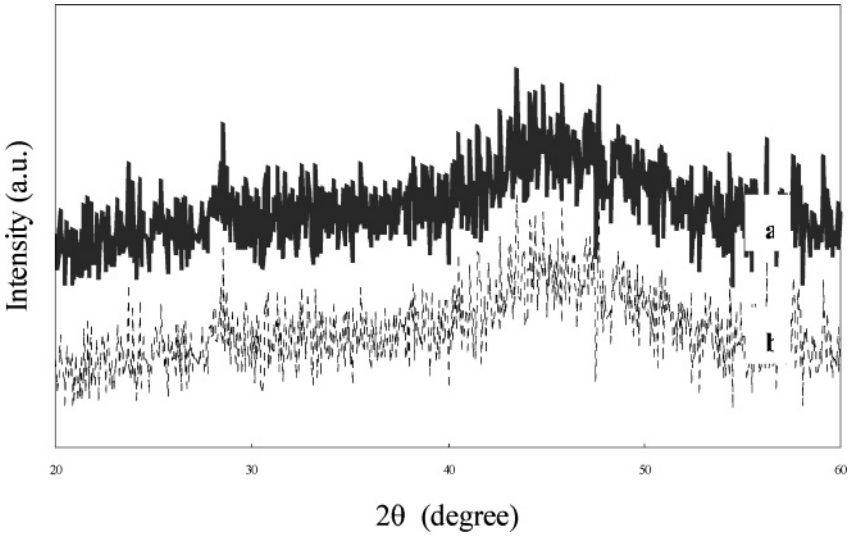

Figure 1. XRD patterns of NiPB samples. (a) NiB(1:3) and (b) NiPB(1:1:3).

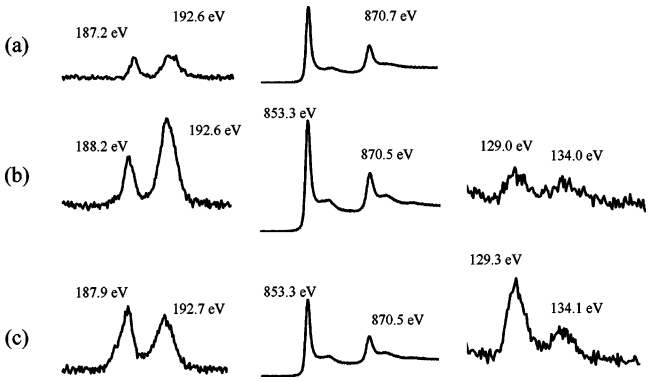

Figure 2. XPS spectra of NiPB catalysts. (a) NiB(1:3), (b) NiPB(1:0.3:3), and (c) NiPB(1:1:3).

In the P_{2P} level, two kinds of phosphorus species appeared on the surface of all the NiPB samples. The peaks around 129.0−129.3 and 134.0−134.1 eV are assigned to phosphorus interacting with nickel and oxidized phosphorus, respectively. In comparison with the binding energy of red phosphorus (130.4 eV), the binding energy of all the NiPB samples (129.0−129.3 eV) shifted negatively by 0.7−0.9 eV, indicating that the phosphorus combined with nickel metal in the NiPB samples was found to accept electrons from the nickel metal.

Observing the area under the curve, there is no obvious difference in the Ni_{2p} spectra. Only the capacity of nickel in the sample NiPB(1:0.3:3) is more than the others, no matter if it is elemental nickel or oxidized nickel. On the B_{1s} spectrum, the content of boron is NiPB(1:0.3:3) > NiPB(1:1:3) > NiB-(1:3). This result is in accords with the results of the ICP-AES analysis. The boron content of NiPB(1:0.3:3) is the most, but among it, 79% is oxidized boron. In the sample NiPB(1:1:3), the elemental boron is in the majority (50.44%). In the sample NiB(1:3), the content of oxidized boron (58.82%) is more than that of elemental boron (41.18%). There are two peaks around 192.60 eV, indicating that there are two kinds of oxidized boron. On the P_{2p} spectrum, the content of phosphorus in NiPB(1:1:3) is undoubtedly more than that in NiPB(1:0.3:3). However, the content of elemental phosphorus is 2.1 times that of oxidized phosphorus in the sample NiPB(1:1:3), and the content of elemental phosphorus is 1.6 times of oxidized phosphorus in the sample NiPB(1:0.3:3).

In this study, the amount of phosphorus has obviously influenced the particle sizes and compositions of the catalysts. The change between elemental and oxidized states was also under the influence. However, no reliable trend was found since the samples were easily oxidized when exposed to air. Nevertheless, the presence of phosphorus could increase the surface area and boron content of the catalysts.

3.2. Catalytic Activity. The catalytic system in a slurry reactor involves processes such as gas-to-liquid mass transfer, liquid-to-particle mass transfer, intraparticle diffusion, adsorption, surface reaction, and desorption of products.[14] To evaluate the extent of mass-transfer limitations related to diffusion from the liquid to the solid phase and within the catalyst particle, the methods introduced by Carberry,[40] Wheeler,[41] and Weisz and Prater[42] have been adopted. Gas−liquid mass-transfer limitation can be eliminated by the proper stirring speed.[41] A series of experiments has been done. The results showed that the conversion would not change if the stirring speed was faster than 400 rpm. Therefore, the stirring speed was fixed at 500 rpm in this study. Since the catalyst particle was very fine, it was expected that the intraparticle diffusion resistance could be neglected.[41] Using the criteria mention previously, the results also confirmed that the experiments were conducted in the reaction-controlled regime.

The catalytic activities of these catalysts were tested by *p*-CNB hydrogenation. In this study, *p*-chloroaniline (*p*-CAN) was the primary product on all NiPB catalysts. The selectivity to *p*-CAN on all catalysts was greater than 99%.

Figure 3 shows the time-conversion curves of *p*-CNB on the NiPB catalysts. It shows that the reaction is first order with respect to *p*-CNB. There was an induction period in the initial period that is due to the re-reduction of the catalyst. The presence of phosphorus changed the catalytic activity of the NiB catalyst. Because of the different transference between nickel metal and metalloids, phosphorus draws electrons and boron donates electrons, which results in a markedly different hydrogenation activity. Adding a suitable amount of phosphorus can increase the activity of the catalyst. However, overdoses of phosphorus decreased the activity of the catalyst. The samples NiPB(1:0.3:3) and NiPB(1:1:3) had similar hydrogenation activities at 393 K, and both were very active. The conversion of *p*-CNB on NiPB(1:0.3:3) and NiPB(1:1:3) achieved 70% within 10 min and 97% in 20 min. To magnify the difference between NiPB(1:0.3:3) and NiPB(1:1:3), the reaction temperature was lower down to 353 K. The results at 353 K showed that NiPB(1:0.3:3) was more active than NiPB(1:1:3). The

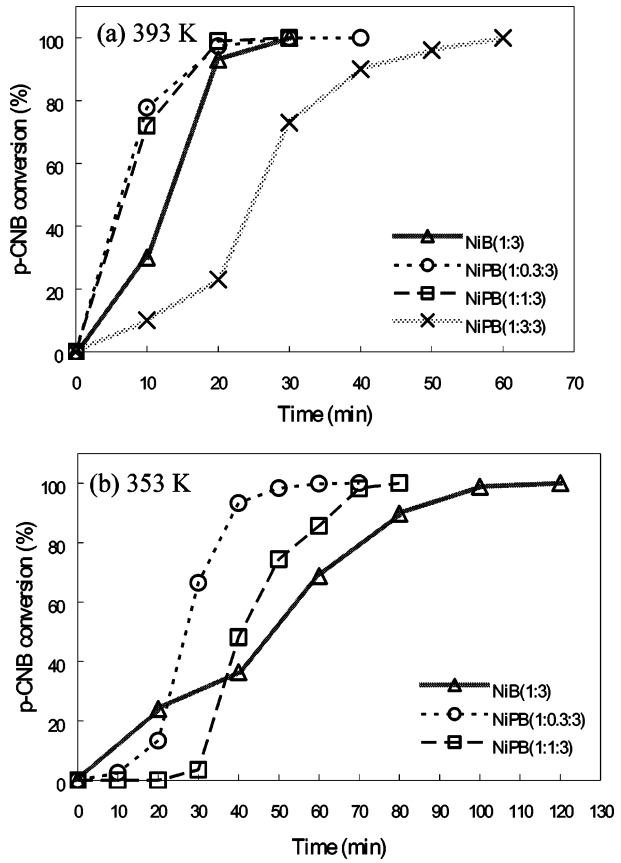

Figure 3. Time-conversion curves of *p*-CNB hydrogenation on NiB and NiPB catalysts. (a) Reaction temperature 393 K and (b) reaction temperature 353 K. □ NiB(1:3); ■ NiPB(1:0.3:3); ▲ NiPB(1:1:3); and □ NiPB(1:3:3). (Reaction condition: 1.2 MPa hydrogen pressure, absolute ethanol as the reaction medium, 500 rpm stirring speed, 0.2 M *p*-CNB, and 2 mmol Ni catalyst.)

conversion of *p*-CNB on NiPB(1:0.3:3) was >90% within 40 min. Instead, NiPB(1:1:3) only achieved 50% at 40 min. Figure 3 also demonstrates that the activity of the NiPB catalysts decreased in the order of NiPB(1:0.3:3) > NiPB(1:1:3) > NiB-(1:3) > NiPB(1:3:3). The sample NiPB(1:3:3) had the lowest activity, and it was caused by the excessive phosphorus. The results clearly demonstrated that NiPB catalysts prepared with suitable Ni/P/B ratios in the starting materials had higher activities than NiB catalysts. However, overdoses of phosphorus would cause the decrease in activity. In a parallel study, the NiP catalyst showed no activity at 120 °C under the same reaction conditions. This confirmed that small amounts of phosphorus in the NiB catalyst can increase the surface area and turnover frequency. Both are beneficial for promoting the reaction. However, overdoses of phosphorus became a poison for the Ni catalyst.

Table 2 lists the activities of the hydrogenation of *p*-CNB to *p*-CAN catalyzed by nanosized NiB and NiPB amorphous alloy catalysts. The order of catalytic activity per weight of the catalyst was NiPB(1:0.3:3) > NiPB(1:1:3) > NiB(1:3) > NiPB(1:3:3). The specific catalytic activity per surface area was also in the same order, indicating that the surface area is not the only reason for the difference in reaction rates. The differences among the catalytic activities can also be attributed to the difference of the electron density on the nickel metal among NiB and NiPB catalysts.[14−16,39] In the NiPB catalysts, the different electron transference between nickel and metalloid (B and P) (boron donates electrons to nickel and phosphorus draws electrons from nickel) exists at the same time. One can regulate the electron

Table 2. Initial Activities of NiB and NiPB Catalysts in Hydrogenation of *p*-CNB[a]

	activity	
catalyst	μmol (m^2 cat)$^{-1}$ s^{-1}	μmol (g cat)$^{-1}$ s^{-1}
NiB(1:3)	73.26	3.99
NiPB(1:0.3:3)	95.20	5.25
NPB(1:1:3)	79.36	4.60
NiPB(1:3:3)	59.52	3.83

[a] Reaction conditions: 1.2 MPa hydrogen pressure, 393 K reaction temperature, absolute ethanol as the reaction medium, 500 rpm stirring speed, 0.2 M *p*-CNB, and 2 mmol Ni catalyst.

Table 3. Turnover Frequencies (TOF) and Activation Energies of NiB and NiPB Catalysts[a]

	TOF[b] (1/site s)		
catalyst	TOF_{353K}	TOF_{393K}	activation energy (kJ/mol)
NiB(1:3)	0.072	0.155	22.11
NiPB(1:0.3:3)	0.114	0.204	16.78
NPB(1:1:3)	0.098	0.179	17.39
NPB(1:3:3)	0.074	0.149	20.18

[a] Reaction conditions: 1.2 MPa hydrogen pressure, 353 and 393 K reaction temperature, absolute ethanol as the reaction medium, 500 rpm stirring speed, 0.2 M *p*-CNB, and 2 mmol of Ni catalyst. [b] *TOF* = (mol of reactant/g of Ni s)/(mol of Ni on surface/g of catalyst).

density of nickel by regulating the concentrations of boron and phosphorus in the catalysts.

Table 3 lists the turnover frequencies (TOFs) and the activation energies of hydrogenation of *p*-CNB catalyzed by NiB and NiPB amorphous alloy catalysts. The TOF of the catalyst was calculated by the surface area of 6.5×10^{-20} m^2 per Ni atom, based on an average of the areas for the (1 0 0), (1 1 0), and (1 1 1) planes. The surface area of nickel metal can be calculated by subtraction of boron and phosphorus areas from the BET surface area of the catalyst. The TOF value of the catalysts decreased in the order NiPB(1:0.3:3) > NiPB(1:1:3) > NiB(1:3) > NiPB(1:3:3). The TOFs are in the same order as those of a specific activity per surface area because nickel metal is the major component on the surface and the areas of boron and phosphorus per atom are very small.

The activation energy was calculated to be 16.78 kJ/mol for NiPB(1:0.3:3) and 17.39 kJ/mol for NiPB(1:1:3). It demonstrated that NiPB(1:0.3:3) had a lower activation energy to process the hydrogenation. It reconfirmed that the reaction was carried out in a kinetic-controlled regime because the activation energy would be lower if it was in a mass-transfer controlled regime. That the NiB catalyst had the highest activation energy and the longest induction period demonstrated that the addition of phosphorus can effectively improve the reaction rate of the hydrogenation of *p*-chloronitrobenzene with lowering the activation energy. In addition, phosphorus can passivate the catalyst to some extent to prevent the nickel metal from reoxidizing and therefore shortening the induction period. The nanosized NiPB amorphous alloy catalysts, combining the effect of metalloid elements and the features of amorphous structure, demonstrate a markedly higher specific hydrogenation activity in the liquid-phase hydrogenation of *p*-CNB than the NiB catalyst.

4. Conclusion

A series of nanosized NiPB amorphous alloy catalysts with various Ni/P/B ratios was prepared by chemically reacting nickel acetate, sodium hypophosphite, and sodium borohydride in aqueous solution. On the basis of the results presented herein, we could conclude the following: (1) The initial Ni/P/B molar ratios of starting materials affected the concentration of boron

and phosphorus bound to the nickel metal, resulting in a change of surface area, amorphous structure, electronic state of nickel, and hydrogenation activity of the catalyst. (2) The XPS results revealed that boron could donate electrons to the nickel metal and that phosphorus could accept electrons from the nickel metal in the NiPB catalysts. By regulating the concentrations of boron and phosphorus, one could regulate the electron denisity of nickel. (3) The BET surface area of the catalyst increased with an increase of phosphorus content in the NiPB samples. (4) The order of activity per weight of the catalyst was NiPB(1:0.3:3) > NiPB(1:1:3) > NiB(1:3) > NiPB(1:3:3). The specific catalytic activity per surface area and TOF were also in the same order. The high activity of the NiPB catalyst could be attributed to high surface area and high TOF. (5) NiPB catalysts prepared with suitable Ni/P/B ratios in the starting materials had higher activities than the NiB catalyst. Small amounts of phosphorus in the NiB catalyst could increase the surface area and turnover frequency. Both are beneficial for promoting the reaction. However, overdoses of phosphorus became a poison for the Ni catalyst. The presence of phosphorus also could passivate the catalyst and prevent it from reoxidizing the metal, which in turn decreases the induction period in the reaction.

Acknowledgment

This research was supported by Ministry of Economic Affairs, Taiwan, Republic of China under Contract 93-EC-17-A09-S1-022.

Literature Cited

(1) Wonterghem, J. V.; Moyup, S.; Christion, J. W.; Charles, S.; Wells, W. S. *Nature* **1986**, *322*, 622.
(2) Corrias, A.; Ennas, G.; Licheri, G.; Marongiu, G.; Musinu, A.; Paschina, G.; Piccaluga, G.; Pinna, G.; Magini, M. *J. Mater. Sci. Lett.* **1988**, *7*, 407.
(3) Linderoth, S.; Morup, S.; Meagher, A.; Larsen, J.; Bentzon, M. D.; Clausen, B. S.; Koch, C. J.; Wells, S.; Charles, S. W. *J. Magn. Magn. Mater.* **1989**, *81*, 138.
(4) Linderoth, S.; Morup, S. *J. Appl. Phys.* **1990**, *67*, 4472.
(5) Xue, D. S.; Li, F. S.; Zhou, R. J. *J. Mater. Sci. Lett.* **1990**, *9*, 506.
(6) Jiang, J.; Dezsi, U.; Lin, X. *J. Non-Cryst. Solids* **1990**, *124*, 139.
(7) Shen, J.; Hu, Y. Z.; Zhang, L. F.; Li, Y. Z.; Chen, Y. *Appl. Phys. Lett.* **1991**, *59*, 3545.
(8) Shen, J. Y.; Hu, Z.; Hsia, Y. F.; Chen, Y. *Appl. Phys. Lett.* **1991**, *59*, 2510.
(9) Saida, J.; Inoue, A.; Masumoto, T. *Mater. Sci. Eng. A* **1991**, *133*, 771.
(10) Deng, J. F.; Chen, H. Y. *J. Mater. Sci. Lett.* **1993**, *12*, 1508.
(11) Hu, Z.; Shen, J. Y.; Fan, Y. N.; Hsia, Y. F.; Chen, Y. *J. Mater. Sci. Lett.* **1991**, *12*, 1020.
(12) Shen, J. Y.; Hu, Z.; Zhang, Q.; Zhang, L. F.; Chen, Y. *J. Appl. Phys.* **1992**, *71*, 5217.
(13) Yamashita, H.; Yoshikawa, H.; Funabiki, T.; Yoshida, S. *J. Chem. Soc., Faraday Trans. 1* **1986**, *82*, 1771.
(14) Okamoto, Y.; Nitta, Y.; Imanaka, T.; Teranishi, S. *J. Chem. Soc., Faraday Trans. 1* **1979**, *75*, 2027.
(15) Okamoto, Y.; Nitta, Y.; Imanaka, T.; Teranishi, S. *J. Chem. Soc., Faraday Trans. 1* **1980**, *76*, 998.
(16) Okamoto, Y.; Nitta, Y.; Imanaka, T.; Teranishi, S. *J. Catal.* **1980**, *64*, 397.
(17) Yao, H. C.; Emmett, P. H. *J. Am. Chem. Soc.* **1962**, *84*, 1086.
(18) Ma, A.; Lu, W.; Min, E. U.S. Patent 6,051,528, 2000.
(19) Seo, G.; Chang, H. J. *J. Catal.* **1981**, *67*, 424.
(20) Liu, I. H.; Chang, C. Y.; Liu, S. C.; Chang, I. C.; Shih, S. M. *Atmos. Environ.* **1994**, *28*, 3409.
(21) Li, C.; Chen, Y. W.; Wang, W. J. *Appl. Catal., A Gen.* **1994**, *119*, 185.
(22) Shen, J.; Hu, Z.; Zhang, Q.; Zhang, L.; Chen, Y. *J. Appl. Phys.* **1992**, *71*, 5217.
(23) Lee, S. P.; Chen, Y. W. *Ind. Eng. Chem. Res.* **2001**, *40*, 1495.
(24) Baiker, A. *J. Chem. Soc., Faraday Discuss.* **1989**, *87*, 239.
(25) Molnar, A.; Smith, G. V.; Bartok, M. *Adv. Catal.* **1989**, *36*, 329.
(26) Deng, J. F.; Li, H.; Wang, W. J. *Catal. Today* **1999**, *51*, 113.
(27) Chen, Y. *Catal. Today* **1998**, *44*, 3.
(28) Yoshida, S.; Yamashita, H.; Funabiki, T.; Yonezawa, T. *J. Chem. Soc., Chem. Commun.* **1982**, 964.
(29) Yoshida, S.; Yamashita, H.; Funabiki, T.; Yonezawa, T. *J. Chem. Soc., Faraday Trans. 1* **1984**, *80*, 1435.
(30) Yamashita, H.; Funabiki, T.; Yoshida, S. *J. Chem. Soc., Chem. Commun.* **1984**, 868.
(31) Yamashita, H.; Yoshikawa, M.; Funabiki, T.; Yoshida, S. *J. Chem. Soc., Faraday Trans. 1* **1985**, *81*, 2485.
(32) Lee, S. P.; Chen, Y. W. *Ind. Eng. Chem. Res.* **1999**, *38*, 2548.
(33) Yu, W. W.; Liu, H. *J. Mol. Catal.* **2006**, *243*, 120.
(34) Li, C.; Chen, Y.; Wang, W. J. *Appl. Catal.* **1994**, *119*, 185.
(35) Metcalfe, A.; Rowden, M. W. *J. Catal.* **1971**, *22*, 30.
(36) Yao, H. C.; Emmett, P. H. *J. Am. Chem. Soc.* **1962**, *84*, 1086.
(37) Lee, S. P.; Chen, Y. W. *Stud. Surf. Sci. Catal.* **2000**, *130*, 3483.
(38) Lee, S. P.; Chen, Y. W. *J. Chem. Technol. Biotechnol.* **2000**, *75*, 1073.
(39) Deng, J.; Yang, J.; Sheng, S.; Chen, H. *J. Catal.* **1994**, *150*, 434.
(40) Carberry, J. J. In *Catalysic Science and Technology*; Anderson, J. R., Boudart, M., Eds.; Springer-Verlag: Berlin, 1987; Vol. 8, p 131.
(41) Wheeler, A. *Advances in Catalysis*; Academic Press: New York, 1951; Vol. 3, p 249.
(42) Weisz, P. B.; Prater, D. C. *Advances in Catalysis*; Academic Press: New York, 1954; Vol. 6, p 143.
(43) Fogler, H. S. *Elements of Chemical Reaction Engineering*; Prentice Hall: Englewood Cliffs, NJ, 1992.

Received for review May 9, 2006
Revised manuscript received September 29, 2006
Accepted October 13, 2006

IE0605736